Selection and characterization of specific nanobody against neuropilin-1 for inhibition of angiogenesis

Shamsi Naderi, Reyhaneh Roshan, Hajarsadat Ghaderi, Mahdi Behdani, Sara Mahmoudi, Mahdi Habibi-Anbouhi, Mohammad Ali Shokrgozar, Fatemeh Kazemi-Lomedasht

Selection and characterization of specific nanobody against neuropilin-1 for inhibition of angiogenesis

Shamsi Naderi[1], Reyhaneh Roshan[1], Hajarsadat Ghaderi[1], Mahdi Behdani[1**], Sara Mahmoudi[1] , Mahdi Habibi-Anbouhi[2], Mohammad Ali Shokrgozar[2], Fatemeh Kazemi-Lomedasht[1*].

[1]Venom and Biotherapeutics Molecules Laboratory, Biotechnology Department, Biotechnology Research Center, Pasteur Institute of Iran, Tehran, Iran

[2]National Cell Bank of Iran, Pasteur Institute of Iran, Tehran, Iran

[*]corresponding author: Fatemeh Kazemi-Lomedasht, Biotechnology Research Center, Venom and Biotherapeutics Molecules Laboratory, Pasteur Institute of Iran, Tehran, Iran. (T) 982166480780 (E)

fa_kazemi@pasteur.ac.ir

** Co-Corresponding author: Mahdi Behdani, Biotechnology Research Center, Venom and Biotherapeutics Molecules Laboratory, Pasteur Institute of Iran, Tehran, Iran. (T) 982166480780 (E)

behdani@pasteur.ac.ir

Abstract

Neuropilin-1 (NRP-1), non-tyrosine kinase receptor, was initially identified as axonal protein and later recognized as co-receptor for vascular endothelial growth factor (VEGF). Neuropilins (NRPs) are involved in vascular development and tumor angiogenesis. Over the last years, many studies have been accomplished to inhibit angiogenesis. In this study, the nanobody library was panned against immobilized NRP-1 antigen. High affinity and specificity nanobodies were selected through monoclonal ELISA. The selected nanobodies inhibited proliferation and tube formation of HUVEC and MCF-7 cells *in vitro* and *ex vivo*. The results highlight potential of anti-NRP1 nanobodies in inhibition of angiogenesis both *in vitro* and *ex vivo* and promises development of novel therapeutics against pathologic angiogenesis.

Key words: VEGF, NRP-1, Nanobody, Angiogenesis.

1. Introduction

Neuropilin (NRP), as cell surface receptor, plays important role in cell survival, migration and angiogenesis. NRPs with 40% identity at the amino acid level, are conserved in all

vertebrates(1). NRP-1 is a type I transmembrane receptor with molecular weight of 120–140 kDa. NRP-1 is a homodimer receptor which is involved in binding to extracellular ligands including some isoforms of vascular endothelial growth factor (VEGF), fibroblast growth factor (FGF) , transforming growth factor beta (TGF-β), hepatocyte growth factor (HGF) and class 3 semaphorins (2). The most studied interaction of the NRP-1 (which works as co-receptor with VEGFR1/2) is with $VEGF_{165}$ that result in angiogenesis, invasion, and metastases of tumor cells. NRP-1 enhances transduction of biological signals in endothelial cells by binding of VEGF-A to VEGFR2(3). In addition, NRP-1 mediates tumor development and angiogenesis. It has been considered that increased expression of NRP1 correlated with more invasive and advanced stage of cancer. Several inhibitors including small molecules, siRNA, and monoclonal antibodies, have been evaluated against NRP-1 (4, 5). For instance, in a study, it has been found that blocking of NRP-1 function enhanced the antitumor effects of anti-VEGF-A antibody in mouse xenograft models by preventing VEGF-A binding to NRP-1(6). In addition to the VEGF-mediated pathway, other growth factors like FGF, platelet-derived growth factor (PDGF), HGF and receptors may interact with NRP-1 on tumor cells to stimulate angiogenesis and tumor progression(7). During the last decades, monoclonal antibodies (mAbs) have been developed against cancer-associated membrane proteins, or their ligands. Nevertheless, therapeutic application of mAbs especially in blocking tumor angiogenesis, have been limited by their complexity and large size in clinical. To overcome this obstacle, attractive strategies such as miniaturization of the antibodies have been conducted (8, 9). Discovery of antibodies devoid of light chains, VHHs or Nanobodies®, in *dromedaries* have been revealed several advantages for biotechnological applications. Nanobodies have small size (~15 kDa), a high stability and solubility and express comfortably in microorganisms. Furthermore, they have high penetration rate into tissues that make them appropriate candidate for therapy (10, 11). The purpose of this study was to establish anti-NRP-1 nanobodies in order to inhibit angiogenesis. In this study, anti-NRP-1 nanobodies have been isolated using phage display and their characteristic and functionality have been evaluated.

2. Materials and methods

2.1. Materials

Monoclonal anti-hemagglutinin antibody(anti-HA), anti-mouse HRP conjugated antibody, and anti-M13-HRP antibody were purchased from Roche, Switzerland. HRP-conjugated anti-His tag antibody was purchased from cytomatingen.VCSM13 helper phage was purchased from Amersham-Pharmacia. NRP-1-Fc chimera antigen and other antigens used in this study were obtained from R&D Systems. The pHEN-4 and pHEN-6c vectors gifted by Serge Muyldermans (Laboratory of Cellular and MolecularImmunology, Vrije University Brussels, Brussels, Belgium). BSA, Casein, and Skim milk were purchased from Merck. Maxisorp 96-well plate was purchased from Roskilde. Protein marker was purchased from Sinaclon, Iran. Immobilized- metal affinity chromatography resin was purchased from Qiagen, Germany. HUVEC, MCF-7 and HEK cells were purchased from cell bank of Pasteur Institute of Iran. All of reagent for cell culture and GeltrexTMLDEV-Free Reduced Growth Factor Basement Membrane M were purchased from Gibco. All other reagents used in this study were purchased from Sigma.

2.2. Preparation of nanobody library

The nanobody library preparation method for anti-NRP-1 was similar to protocol used for previous work by our team (12). Briefly, a young camel (*Camelus dromedarius*) was immunized with NRP-1 antigen. Immune reponses against NRP-1 was checked by ELISA and peripheral blood mononuclear lymphocytes (PBMCs) were isolated and total RNA was extracted. The cDNA was synthesized and VHH gene was amplified by two consecutive PCR. The VHH gene was digested with *Pst* I and *Not* I restriction enzymes. The digested VHHs were ligated into linear pHEN-4 vector which was digested by the same restriction enzymes. Therefore, the recombinant phagemids were transformed into electrocompetent *E. coli* TG1 cells (12).

2.3. Biopanning of the nanobody library

An amplified nanobody library containing 10^7 clones was infected with 10^7 colony forming units (c.f.u) of VCSM13 helper phage. In this way, phage particles displaying nanobodies were rescued and biopanning was performed against immobilized NRP-1 antigen. To capture NRP-1 specific phages, four subsequent rounds of biopanning were performed. Briefly, a 96-well plate was coated overnight at 4 ˚C with 100 µl of NRP-1(0.5 µg/mL) as target antigen and phosphate-buffered saline (PBS) as negative control. The next day, the plate was washed with PBS and blocked with 4% skimmed milk in PBS (MPBS) at RT for 1h. About 10^9 cfu of

phage particles were incubated for 1h with the human- full Fc (1 mg/ml in PBS) with gentle mixing to eliminate Fc-bounded phage particles. The next, supernatant transferred to a negative well containing PBS at RT for 1 h. Then, supernatant was transferred from the negative well to antigen-coated well and incubated at RT for 1 h. The wells were washed 5 times with PBST (0.05% (V/V) Tween 20 in PBS). The bounded phages eluted by adding of 100µl triethylamine(TEA, pH 10.0, 100 mM) for 10 min, and then neutralized by 100µl Tris–HCl (pH 8.0, 1M). Eluted phages (output) were used for titration and for infection of 5 ml of *E. coli* TG1 (OD_{600nm} 0.4- 0.6). By adding of VCSM13 helper phage, phages were rescued and subsequently precipitated in PEG/NaCl (PEG/NaCl (20% polyethylene glycol 6000/2.5 M NaCl in water). Then phages were centrifuged and the pellet was resuspended in PBS (input) and used for subsequent rounds. The next rounds of panning were performed as mentioned above with more stringent washing by enhancing the amount of Tween 20 in PBST solution (0.05%, 0.1%, 0.2%, and 0.4%). To evaluate enrichment of panning rounds, TG1 cells (OD_{600} 0.4-0.6) were infected with serially diluted of input phages and then infected cells were plated on a 2XTY plate containing 100 µg/mL ampicillin. Colonies were counted at each round and the result of each round was identified.

2.4. Polyclonal phage ELISA

The maxisorp 96-well plate was coated with the NRP-1 antigen (1 µg/ml) overnight at 4 °C. In addition, for detection of non-specific binding, BSA and human- full Fc was used as control wells. The next day, coating solution was discarded and the plate was washed with PBST and then blocked with MPBS for 1h at RT. Then wells were washed and 10^{12} cfu of output phages were added to the wells and incubation was performed at RT for 1 h. After washing, the anti-M13-HRP antibody (1:2000) was added and incubated at RT for 1 h. Finally, TMB (3,3′, 5,5′-tetramethyl benzidine) was added and the reaction was stopped by adding 2 N H2SO4. The absorption was measured by ELISA reader at 450 nm.

2.5. Periplasmic extract ELISA (PE-ELISA)

Individual *E. coli* TG1colonies were randomly selected by infecting of bacteria with eluted phages as above mentioned and grown in 1 ml of TB medium to reach log phase (OD_{600} 0.4-0.6). Production of nanobody containing a haemaglutinin (HA) tag in the periplasme of *E. coli* was induced with 1 mM isopropyl D-1-thiogalactopyranoside (IPTG). Expression of

nanobody was identified with ELISA. The bounded nanobodies to coated antigen in 96-wells plate, were detected using anti-HA antibody (1:2000) followed by anti-mouse HRP conjugated antibody (1:5000). Then TMB substrate was added and absorbance was measured at 450 nm. Finally, positive clones were then sequenced to identify the specific nanobody genes. The 3D structures of nanobodies predicted by Iterative Threading ASSEmbly Refinement (I-TASSER) method(13). Interaction between nanobodies and NRP-1 was evaluated using Hex software (9, 14-16).

2.6. Expression and purification

The specific nanobody genes were amplified using forward; 5_GATGTGCAGCTGCAGGAGTCTGGGGGAGG_3 and reverse primers; 5_GGACTAGTGCGGCCGCTGGAGACG-GTGACCTGGGT _3. Amplified nanobody gene sub-cloned into pHEN-6c bacterial expression vector containing c-terminal His6 tag using the *BstE* II and *Pst* I restriction enzymes. The recombinant pHEN-6c construct was transformed into *E. coli* WK6 cells. The transformants were confirmed by colony-PCR. Transformants were grown in 330 ml of 2XTY medium in baffled flask. Nanobody expression was induced in periplasmic space of the *E. coli* cells by 1 mM IPTG. Periplasmic expressed proteins were released using osmotic shock. Recombinant proteins then were purified by immobilized metal affinity chromatography resin with 500 mM imidazole. Ultimately, the eluted protein was dialyzed against PBS with 5 kDa cutoff(17).

2.7. Polyacrylamide gel electrophoresis analysis

The SDS-PAGE was carried out under reducing condition on 12% gel. After then, Coomassie Blue stain was used to stain the protein bands in polyacrylamide gel. The next, identification of nanobodies were evaluated by western blot using HRP-conjugated anti-His tag antibody (1:2000). Finally, the nanobody bands were exposed by 3, 3′-diaminobenzidine substrate (DAB). The concentration of nanobodies were determined by assessment of UV absorption at 280 nm(18, 19).

2.8. Specificity of nanobodies

The specificity and cross-reactivity of selected nanobodies were examined with the following antigens by ELISA. One µg/mL of antigens such as BSA, casein, skim milk, epithelial cell

adhesion molecule (EpCAM), programmed cell death protein 1 (PD-1), programmed death-ligand 1 (PDL-1), cytotoxic T-lymphocyte–associated antigen 4 (CTLA-4) , and zinc transport protein LIV-1 were coated onto 96-well ELISA plates. In this experiment, bounded nanobodies to the wells were identified by HRP conjugated anti-His antibody followed by HRP substrate.

2.9. Affinity of nanobodies

Affinity of nanobodies were estimated by the method described by Beatty et al(20). Briefly, 100 µl of two different concentrations (1 and 10µg/ml) of NRP-1 antigen and BSA as negative control was coated on 96-well plate. After blocking, wells were incubated for 1 h with increasing concentrations (0–100 nM) of nanobodies. Detection of binding was evaluated by anti-His HRP conjugated antibody (1:1000) followed by TMB substrate. Finally, The affinity constant (K_{aff}) of the nanobodies to the NRP-1 was calculated using the following equation:

$$[Ag]/[Ag'] = N$$

$$kaff = N - 1/2(N[Nb] - [Nb'])$$

2.10. Competitive ELISA assay

To examine ability of NRP-1 specific nanobodies to detect the solution form of NRP-1, a competitive ELISA was designed. In this experiment, 1µg/ml of NRP-1 antigen or BSA as negative control were coated in 96 well microplate and incubated at 4 ˚C overnight. Then, 1µg/ml of nanobodies were incubated with increasing concentrations (0-1 µg/ml) of NRP- 1 for 1 h at 37 °C and then added to the wells coated with NRP-1. The wells incubated for 1 h. The next, the wells were washed and bounded nanobody to immobilized NRP-1 was detected by ELISA.

2.11. Cell lines

MCF-7 (human breast cancer cell line) and HEK293 (human embryonic kidney) were cultured in Dulbecco's Modified Eagle's Medium (DMEM). Human umbilical vein endothelial cell line (HUVEC) was grown in HAMS-F12. All of the culture media were supplemented with 10% heat inactivated fetal bovine serum (FBS), 100 units/ml penicillin

and 100 µg/ml streptomycin. Cells were detached by a one or three- min exposure to 0. 05% w/v trypsin –EDTA.

2.12. *In vitro* assay

2.12.1. MTT assay

To investigate the anti-proliferative effect of nanobodies, colorimetric assay was performed using a 3-(4, 5-dimethylthiazol-2-yl)-2,5-diphenyltetrazolium bromide (MTT). Briefly, MCF-7, HUVEC and HEK cells (as negative control) were seeded (3×10^3 cells/well) in a 96-well plate. Then cultures were grown for 24 and 48 h and then treated with culture medium containing different concentrations (0 – 20 nM) of nanobodies, or PBS as control. The next, 10 µl MTT solution (5 mg/ml) was added to each well and incubated for 4 h at 37 ˚C. The medium was removed and MTT-formazan crystals solubilized by 100 µl of dimethylsulfoxide (DMSO). Finally, the absorbance was determined by spectrophotometer at 570 nm using a reference wavelength of 630 nm.

2.12.2. Tube formation assay

In this experiment,GeltrexTMLDEV-Free Reduced Growth Factor Basement Membrane M solution was thawed on ice. Fifty µl of Geltrex were transferred into 96-well plate. The plate was incubated in 37 ˚C for 30 min. About 100 µl HAMS-F12 medium supplemented with FBS containing 10^4 HUVEC cells were added on Geltrex. Then, diluted nanobodies was added to the wells. In addition, cells treated with BSA was considered as control. After incubation at 37 ˚C, capillary like structures and endothelial tube formation was observed during 1 to 6 h under inverted microscope. Branching or capillary like structures of the cells were analyzed by Image J software.

2.13. *Ex vivo* assay:

2.13.1. Chicken chorioallantoic membrane model

To investigate anti-angiogenesis activity of selected nanbodies *ex vivo*, chicken chorioallantoic membrane (CAM) was performed. Briefly, fertilized chicken eggs incubated at 37 ˚C with 70% humidity. Six days after, the contents of the eggs were transferred into the petri dish under sterile condition. The embryo and the yolk vessels located on top of an undamaged yolk. Then, discs containing concentrations of nanobody (at the IC50) or 10 µl

PBS as negative control were placed on the top of the embryo and petri dish was transferred to the incubator for 48 h. Finally, inhibition of vessel growth was observed macroscopically.

2.14. Statistical analysis

Statistical analyses were performed by Prism 8.0 Software (GraphPad, San Diego, CA). *P* values < 0.05 was considered statistically significant.

3. Result

3.1. Selection of anti-NRP-1 phages

Four rounds of panning were performed to identify NRP-1specific nanobodies. To evaluate the enrichment of NRP-1 specific phages, the number of output and input phages were compared at each round. The increasing ratio was observed in third and fourth round of biopanning that was 6.3 and 19.4 fold, respectively (Table 1). In addition, to confirm success of selection process, specific bounding of each eluted phage from different round of biopanning was performed by polyclonal phage ELISA. The highest signals were observed in the third and fourth round of panning (Fig. 1). To screen monoclonal phages, over 100 clones were infected with output phages of the third and fourth round of biopanning. Monoclonal phage ELISA results showed that four clones specifically reacted with NRP-1 (Fig. 2). Finally, selected clones were sequenced and alignment was performed by NCBI BLAST tools and the results showed at least 89% homology with VHH sequence of *Camelus dromedaries*. The amino acid sequences of selected nanobodies are shown in Table 2. The predicted 3D structures of nanobodies are shown in Fig 3. Docking was performed to identify protein-protein interaction between nanobodies and NRP-1. In docking, NRP-1 considered as receptor and Nanobodies were to be ligand (Table 3).

3.2. Expression and purification of soluble nanobodies

To generate soluble nanobodies, the nanobodies-encoding genes were sub-cloned into the pHEN-6c expression vector and transformed into *E. coli* WK6 cells. The His-tagged fusion nanobodies were purified by nickel affinity chromatography (Ni^{+}-NTA). Fractions containing each nanobody independently was pooled and dialyzed against PBS1×. The purity of the nanobodies was verified using SDS-PAGE (Fig. 4 A). Western blot analysis was performed using anti-His conjugated HRP and successful expression was confirmed with a band with approximately 17 kDa (Fig. 4 B). The yield of purified nanobodies depending to clones was variable from 0.04–0.07 gram per liter of culture.

3.3. Binding specificity

To determine the specificity of nanobodies, binding of anti-NRP-1 nanobodies to NRP-1 and different proteins were investigated by ELISA. The results indicated that four nanobodies showed significantly high signal in ELISA in comparison with the control proteins (Table4).

3.4. Affinity results

The affinity constant of nanobodies were determined by ELISA, according to the Beatty et al. method (Fig. 5). The K_{aff} of nanobodies are shown in Table 5.

3.5. Competition assay

The results of ELISA showed that binding of selected anti-NRP-1 nanobodies to immobilized NRP-1 was inhibited by binding of nanobodies to solution NRP-1. At increasing concentration of NRP-1, and in the presence of 1 μg/ml NRP-1, nanobodies bounded to soluble antigen and inhibited binding to immobilized antigen. As the result show in Figure 6, the OD values of, Nb16, Nb48 and Nb53 nanobodies were decreased considerably when the concentration of soluble antigen NRP-1 was increased in solution.

3.6. Inhibition of cell proliferation by NRP-1 specific nanobodies

To evaluate concentration-dependent cytotoxic effect of NRP-1 specific nanobodies, MTT assay was performed using MCF-7, HUVECs and HEK cells. It has been shown that after 1 and 2 days incubation period with NRP-1 specific nanobodies, the rate of cell viability decreased significantly ($P < 0.05$) in HUVECs and moderately in MCF-7 cells in a concentration-dependent manner whereas the HEK cells remained unaffected (Fig. 7). The IC50 value in HUVEC cells was 4 and 48 nM in Nb48 and Nb53, respectively and >50 nM in Nb2 and Nb16. In addition, the IC50 value in MCF-7 cells was18 and 69 nM in Nb48 and Nb53, respectively and >70 nM in Nb2 and Nb16.

3.7. Tube formation assay

To study whether the NRP-1 is involved in progress of angiogenesis, we used selected nanobodise toward NRP-1. Results showed that incubation of HUVECs with Nb 48 (at IC50 concentration), significantly decreased tube length of the cells (Fig. 8). The Nb48 attenuated tube formation by ~46% compared to HUVECs untreated as control (Fig. 9). The other Nbs showed a slightly effect on total length. These results demonstrated that NRP-1 receptors might be involved partially in tube formation of HUVECs.

3.8. CAM assay

To evaluate the anti-angiogenic responses of the selected nanobodies, CAM assay was performed. After 48h, the Nb48 significantly inhibited the development of angiogenesis. The other naobodies, Nb2, Nb16 and Nb 53 slightly inhibited growth of the vessels (Fig. 10). In the control group treated with only PBS there was not observed any anti-angiogenic effect.

4. Discussion

The purpose of the present study was to generate and characterize specific nanobodies against NRP-1. Previous studies have been demonstrated that NRP-1 plays an essential role in tumor angiogenesis, and metastasis and is considered as a promising candidate for cancer therapy (21). Currently, a few anti-angiogenic agents have been approved by FDA that could inhibit VEGF pathway. However, resistance to anti-angiogenic drugs may limit therapy in patients and lead to disease progression(22). In this study, anti-NRP-1 nanobodies were isolated and successfully characterized by phage display method. Phage display technology is a fundamental drug discovery technology in identification of antibodies(23). To obtain nanobodies with high affinity and specificity(24) toward NRP-1 antigen, and eliminate the nanobodies that cross-react with BSA and human full- FC, consequtive rounds of panning was performed with increased stringency. To isolate specific clones to NRP-1, periplasmic extract ELISA was performed. More than 100 randomly selected clones from round 3 and 4 of panning were chosen. Four clones showed strong signals on ELISA. Colony PCR showed that four selected colonies contained an inserted fragment of the nanobodies proper size. Docking simulation results showed strong binding of selected nanobodies to NRP-1. Selected colonies were successfully sub-cloned into expression vector and then soluble nanobodies were investigated further by ELISA. Each clone produced on large scale

and then purified through immobilized metal affinity chromatography (IMAC). Immunoblotting indicated the successful production and purification (>95%) of nanobodies for *in vitro* experiment. Binding affinity for nanobodies was different from 5 to 80 nM. The different binding affinities of the nanobodies to NRP-1 suggest that they may recognize different epitopes on same antigen (12). The most NRP-1 inhibitors mainly targeted VGEF binding to NRP-1. In a study by Pan, Q *et.al,* monoclonal antibodies, anti-$NRP1^{A}$ and anti-$NRP1^{B}$, obtained by naive-antibody phage library and targeted the NRP-1 a1-a2 (Kd= 0.9 nM) and b1-b2 domains (Kd= 0.4 nM), respectively. Both antibodies could inhibit VEGF-dependent endothelial cell migration and angiogenesis *in vitro* (6). The binding specificity of nanobodies were exhibited their desirable reactivity to NRP-1. To determine binding capability of nanobodies in two different phases (solid and solution), competitive ELISA was performed. As immobilized antigens undergo some conformational changes, it may be disturbed antigen recognition in soluble phase (12). In addition, we shown in proliferation assay, Nb48 effectively inhibited HUVEC and MCF-7 proliferation in a dose-dependent manner. However, it had no significant effect on HEK cell proliferation. In a study by Zeng F and et.al, it was found that a monoclonal antibody against NRP-1, significantly reduced the proliferation of MCF-7 cells at 400 µg/ml(25). In addition, we demonstrated that Nb48 effectively inhibited tube formation of HUVECs. Tube formation assay is one of the potential *in vitro* assays for angiogenesis assessment and can be easily perform and quantitative on matrigel(26). Based on our data, we found that Nb48 -treated HUVEC cells significantly decreased the total tube length. Thus, Nb48 may be considered as a functional nanobody candidate to inhibit angiogenesis. Our results suggest that Nb48 have such relative functions. In other study, by phage display screening method, an A7R peptide (ATWLPPR) identified that could bind to NRP1 and partially reduced endothelial cell tube formation (with 500 µM of A7R) (27). In Borriello *et al* study, a potent small molecule could inhibit tubulogenesis by blocking of VGEF-NRP-1 interaction *in vitro* with an IC50 of 0.2µM. The antagonist was able to decrease HUVEC viability by 68% at the IC50 concentration(28). Recent studies have shown that targeting of VGEF-independent NRP-1 may possible a therapeutic potential. It is consider that NRP1 could improve angiogenesis in the absence of VEGFR-1 or VEGFR-2. In a study, targeting with micro RNAs (miRNAs) could regulate NRP-1 expression and reduce angiogenesis *in vitro*(29).

The CAM assay is a frequently applied technique to study angiogenesis. It is cost effective, and is an easily reproducible *ex vivo* model (30). We performed CAM assay to assess the

inhibitory function of nanobodies on tube formation of CAM. Results exhibited the lack of vessel formation in response to anti-NRP-1 nanobody. In a study, development of peptide pTM-NRP1 toward the transmembrane domain of NRP-1 results in maximum inhibition of tube formation (in 10^{-7}M of peptide). In addition, anti-angiogenic effect of peptide was confirmed using *ex vivo* CAM assay(31).

In conclusion, two high affinity and specificity nanobodies were selected from the immune nanobody library by phage display technique. Selected nanobodies efficiently inhibited *in vitro* and *ex vivo* angiogenesis of endothelial cells. The results indicate for potential of selected NRP-1 nanobodies as novel anti-angiogenesis agent.

Acknowledgments

This study was financially supported by Pasteur Institute of Iran. Shamsi Naderi would likes to thank Pasteur Institute of Iran for funding her Ph.D studenship (Ph.D thesis: BP-9476 No)

References

1. Guo HF, Vander Kooi CW. Neuropilin Functions as an Essential Cell Surface Receptor. J Biol Chem. 2015 Dec 4;290(49):29120-6.
2. Leng Q, Woodle MC, Mixson AJ. NRP1 transport of cancer therapeutics mediated by tumor-penetrating peptides. Drug Future. 2017 Feb;42(2):95-104.
3. Djordjevic S, Driscoll PC. Targeting VEGF signalling via the neuropilin co-receptor. Drug Discov Today. 2013 May;18(9-10):447-55.
4. Raskopf E, Vogt A, Standop J, Sauerbruch T, Schmitz V. Inhibition of Neuropilin-1 by RNA-Interference and its Angiostatic Potential in the Treatment of Hepatocellular Carcinoma. Z Gastroenterol. 2010 Jan;48(1):21-7.
5. Jarvis A, Allerston CK, Jia HY, Herzog B, Garza-Garcia A, Winfield N, et al. Small Molecule Inhibitors of the Neuropilin-1 Vascular Endothelial Growth Factor A (VEGF-A) Interaction. J Med Chem. 2010 Mar 11;53(5):2215-26.
6. Pan Q, Chanthery Y, Liang WC, Stawicki S, Mak J, Rathore N, et al. Blocking neuropilin-1 function has an additive effect with anti-VEGF to inhibit tumor growth. Cancer Cell. 2007 Jan;11(1):53-67.
7. Chaudhary B, Khaled YS, Ammori BJ, Elkord E. Neuropilin 1: function and therapeutic potential in cancer. Cancer Immunol Immun. 2014 Feb;63(2):81-99.
8. Arezumand R, Alibakhshi A, Ranjbari J, Ramazani A, Muyldermans S. Nanobodies As Novel Agents for Targeting Angiogenesis in Solid Cancers. Front Immunol. 2017 Dec 8;8.
9. Karami E, Sabatier J-M, Behdani M, Irani S, Kazemi-Lomedasht F. A nanobody-derived mimotope against VEGF inhibits cancer angiogenesis. Journal of Enzyme Inhibition and Medicinal Chemistry. 2020;35(1):1233-9.
10. Harmsen MM, De Haard HJ. Properties, production, and applications of camelid single-domain antibody fragments. Appl Microbiol Biot. 2007 Nov;77(1):13-22.

11. Khodabakhsh F, Behdani M, Rami A, Kazemi-Lomedasht F. Single-domain antibodies or nanobodies: a class of next-generation antibodies. International reviews of immunology. 2018;37(6):316-22.
12. Kazemi-Lomedasht F, Behdani M, Bagheri KP, Habibi-Anbouhi M, Abolhassani M, Arezumand R, et al. Inhibition of angiogenesis in human endothelial cell using VEGF specific nanobody. Mol Immunol. 2015 May;65(1):58-67.
13. Yang J, Zhang Y. Protein structure and function prediction using I-TASSER. Current protocols in bioinformatics. 2015;52(1):5.8. 1-5.8. 15.
14. Pourhashem Z, Yardehnavi N, Behdani M, Kazemi-Lomedasht F. An in silico study to find angiogenesis inhibitory role for Naja oxiana snake venom cytotoxins. 2018.
15. Ahadi M, Behdani M, Shahbazzadeh D, Kazemi-Lomedasht F. In silico docking of matrix metalloproteinase inhibitors of Hemiscorpius Lepturus to human matrix metalloproteinases-opportunities for novel natural therapeutics. 2019.
16. Ahadi M, Ghasemian H, Behdani M, Kazemi-Lomedasht F. Oligoclonal selection of nanobodies targeting vascular endothelial growth factor. Journal of immunotoxicology. 2019;16(1):34-42.
17. Kazemi-Lomedasht F, Muyldermans S, Habibi-Anbouhi M, Behdani M. Design of a humanized anti vascular endothelial growth factor nanobody and evaluation of its in vitro function. Iranian Journal of Basic Medical Sciences. 2018;21(3):260.
18. Sadeghi A, Behdani M, Muyldermans S, Habibi-Anbouhi M, Kazemi-Lomedasht F. Development of a mono-specific anti-VEGF bivalent nanobody with extended plasma half-life for treatment of pathologic neovascularization. Drug testing and analysis. 2020;12(1):92-100.
19. Alirahimi E, Ashkiyan A, Kazemi-Lomedasht F, Azadmanesh K, Hosseininejad-Chafi M, Habibi-Anbouhi M, et al. Intrabody targeting vascular endothelial growth factor receptor-2 mediates downregulation of surface localization. Cancer gene therapy. 2017;24(1):33-7.
20. Beatty JD, Beatty BG, Vlahos WG. Measurement of Monoclonal-Antibody Affinity by Noncompetitive Enzyme-Immunoassay. J Immunol Methods. 1987 Jun 26;100(1-2):173-9.
21. Zeng FW, Luo FH, Lv S, Zhang HP, Cao C, Chen XL, et al. A monoclonal antibody targeting neuropilin-1 inhibits adhesion of MCF7 breast cancer cells to fibronectin by suppressing the FAK/p130cas signaling pathway. Anti-Cancer Drug. 2014 Jul;25(6):663-72.
22. Ferrara N. Pathways mediating VEGF-independent tumor angiogenesis. Cytokine Growth F R. 2010 Feb;21(1):21-6.
23. Nixon AE, Sexton DJ, Ladner RC. Drugs derived from phage display From candidate identification to clinical practice. Mabs-Austin. 2014 Jan-Feb;6(1):73-85.
24. Schreiber G, Keating AE. Protein binding specificity versus promiscuity. Curr Opin Struc Biol. 2011 Feb;21(1):50-61.
25. Zeng F, Luo F, Lv S, Zhang H, Cao C, Chen X, et al. A monoclonal antibody targeting neuropilin-1 inhibits adhesion of MCF7 breast cancer cells to fibronectin by suppressing the FAK/p130cas signaling pathway. Anti-cancer drugs. 2014;25(6):663-72.
26. Arnaoutova I, George J, Kleinman HK, Benton G. The endothelial cell tube formation assay on basement membrane turns 20: state of the science and the art. Angiogenesis. 2009;12(3):267-74.
27. Zhou R, Curry JM, Roy LD, Grover P, Haider J, Moore LJ, et al. A novel association of neuropilin-1 and MUC1 in pancreatic ductal adenocarcinoma: role in induction of VEGF signaling and angiogenesis. Oncogene. 2016;35(43):5608-18.
28. Borriello L, Montès M, Lepelletier Y, Leforban B, Liu W-Q, Demange L, et al. Structure-based discovery of a small non-peptidic Neuropilins antagonist exerting in vitro and in vivo anti-tumor activity on breast cancer model. Cancer letters. 2014;349(2):120-7.
29. Peng Y, Liu Y-M, Li L-C, Wang L-L, Wu X-L. MicroRNA-338 inhibits growth, invasion and metastasis of gastric cancer by targeting NRP1 expression. PloS one. 2014;9(4):e94422.

30. Lokman NA, Elder ASF, Ricciardelli C, Oehler MK. Chick Chorioallantoic Membrane (CAM) Assay as an In Vivo Model to Study the Effect of Newly Identified Molecules on Ovarian Cancer Invasion and Metastasis. Int J Mol Sci. 2012 Aug;13(8):9959-70.
31. Nasarre C, Roth M, Jacob L, Roth L, Koncina E, Thien A, et al. Peptide-based interference of the transmembrane domain of neuropilin-1 inhibits glioma growth in vivo. Oncogene. 2010;29(16):2381-92.

Tables

Table 1: Enrichment results of phage particle after biopanning on NRP-1 antigen.

Rounds of biopanning	No. of colonies in NRP-1 coated well (cfu) (A)	No. of colonies in PBS coated well (cfu) (B)	Enrichment ratio (A/B)
1	201	112	1.8
2	192	96	2
3	182	29	6.3
4	608	31	19.6

Table2: Amino acid sequences of the selected nanobodies. Similar residues are colored as the most conserved one (according to BLOSUM62).

```
                    FR1                 CDR1                FR2          CDR2
Nb16  QVQLVQSGGGSVQAGGSLRLSCvAS-GDTSITVGSGWFRQAPGKEREGVAI-RYMIGVML
Nb48 QVQLVQSGGGSVQAGGSLRLSCAASAGLRAGPIHYGWFRQAPGKEREGVAV--ESDDTAL
Nb2   QVQLVQSGGGSLQAGGSLRLSCAAS-GHERNNYCVGWFRQVPGKEREGVAIFRAGITAVS
Nb53 QVQLVQSGGGSVQAGGSLRLSCAAS-GYERNNYCVGWFRQAPGKEREGVAIFNSGGVSAI

      CDR2                FR3                                CDR3
Nb16  AAQTYTDSVKGRFTISQDNTKNTVYLQMSSLKPEDTAIYYCAAGCVQVRSV-TVPSVY--
Nb48  GFATYADSVKaRFTISQDNTKNTVYLQMNSLKPEDTAIYYCAASI--RRCTWYHPTGYNY
Nb2   GTTYYADSVKGRFTISQDNTKNTVYLQMNSLKPEDTAIYYCTAAkIYPPCT-GISRTYDY
Nb53  QVPYYADSVKGRFTISQDNTKNTVYLQMNSLKPEDTAIYYCCAAkIYPPCT-GISRTYDY

      FR4
Nb16 WGQGTQVYVSS
Nb48 WGQGTQVYVSS
Nb2  WGQGTQVYVSS
Nb53 WGQGTQVYVSS
```

Table 3: Results of docking simulation of nanobodies and NRP-1.

	E. Total	E. Shape	E. Air	Bmp (Bit	Rms (Root

	(kcal/mol)			maps)	mean square)
Nb2	-334/15	-334/15	0	-1	-1
Nb16	-362/13	-362/13	0	-1	-1
Nb48	-347/5	-347/5	0	-1	-1
Nb53	-343/7	-343/7	0	-1	-1

473

474

475 Table4: Specificity of nanobodies. Data display the mean ± standard deviation (SD) of three
476 experiments.

477

Nanobodies	**NRP-1**	**EpCAM**	**CTLA-4**	**LIV-1**	**PD-1**	**PDL-I**	**BSA**	**Skim milk**
Nanobody 2	1.56±0.12	0.46±0.07	0.9±0.17	0.46±0.07	0.61±0.12	0.32±0.08	0.11±0.12	0.12±0.08
Nanobody 16	2.01±0.12	0.51±0.15	0.51±0.12	0.47±0.14	0.42±0.10	0.43±0.10	0.12±0.10	0.13±0.10
Nanobody 48	2.83±0.10	0.32±0.10	0.44±0.15	0.38±0.13	0.31±0.11	0.40±0.08	0.10±0.11	0.10±0.08
Nanobody 53	2.69±0.1	0.26±0.08	0.40±0.11	0.26±0.08	0.22±0.09	0.26±0.11	0.13±0.09	0.12±0.11

478

479 Table 5: Binding affinity of the selected nanobodies to the immobilized NRP-1. The affinity
480 of NRP-1 specific nanobodies were acquired based on the Beatty method. BSA was used as a
481 negative control. The experiments were performed in triplicate, and the data was represented
482 with mean ± SD.

483

Nanobodies	Affinity constant (k_{aff}) nM
Nanobody 2	50
Nanobody 16	5
Nanobody 48	82.5
Nanobody 53	70

484

485

486

Figures

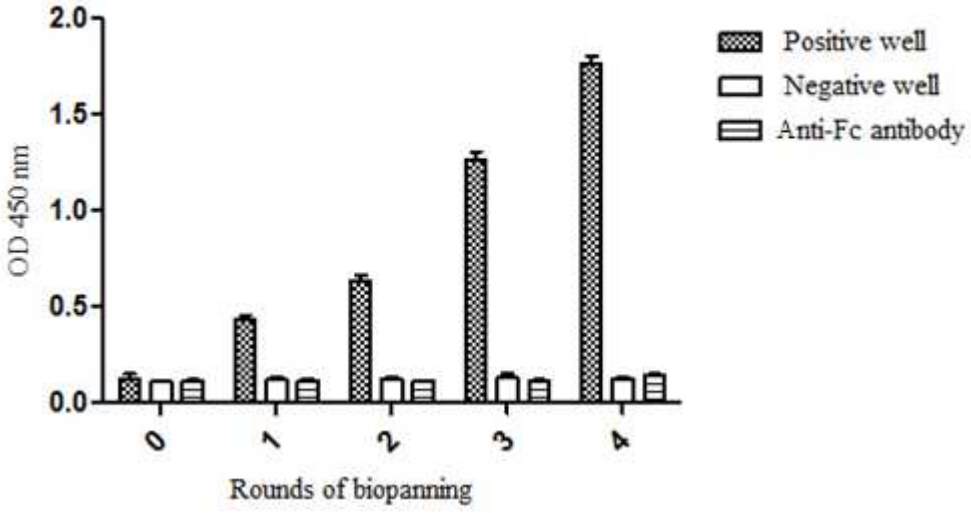

Figure 1. Results of polyclonal phage-ELISA. The assay was performed in triplicate and error bar was considered for mean± standard deviation.

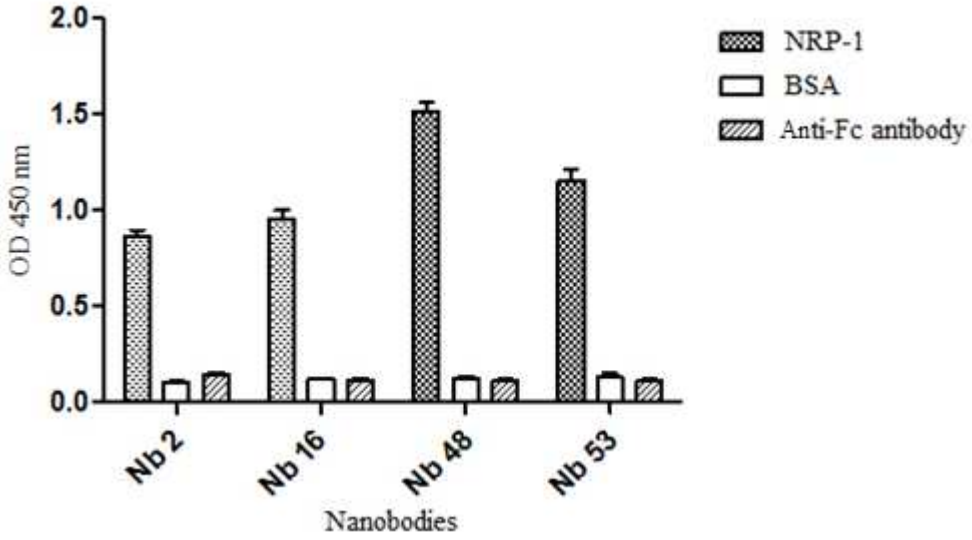

Figure 2. Results of Periplasmic extract ELISA (PE-ELISA). The PE-ELISA showed that four clones specifically reacted with NRP-1 antigen. The graphs display the mean ± standard deviation (SD) of three experiments.

A B

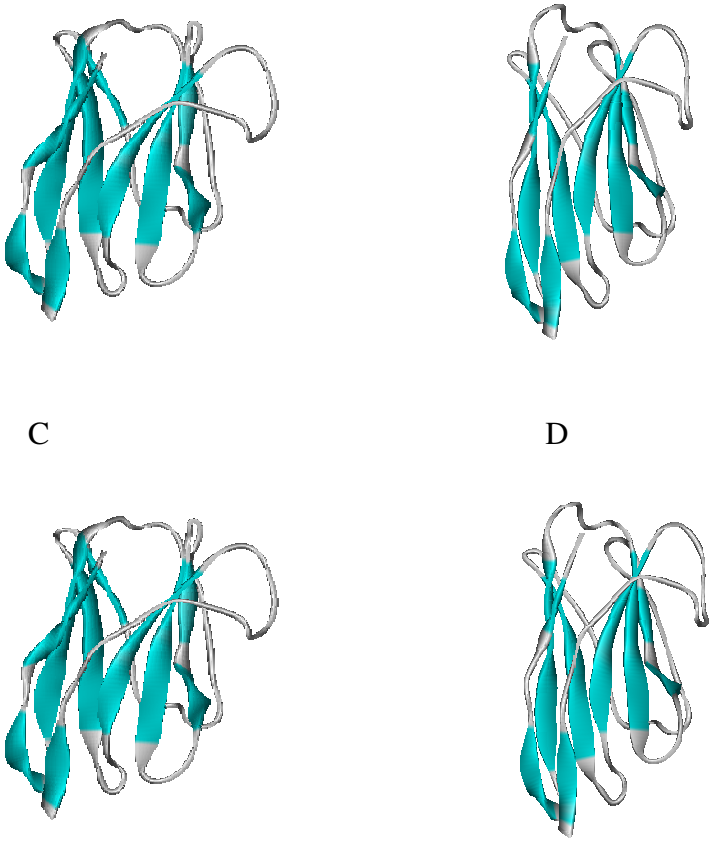

C D

Figure 3. Predicted 3D structure of nanobodies. The 3D structure of nanobodies were predicted by I-TASSER. A; Nb2, B; Nb16, C; Nb48, D; Nb53.

A B

Figure 4. Results of expression and purification of the selected nanobodies. A). SDS-PAGE of purified nanobodies. B) Immunoblotting. M: molecular weight marker, lane 1: Nb2; lane

2: Nb16; lane 3: Nb48. lane 4: Nb53. Detection was done by the HRP conjugated anti -His antibody.

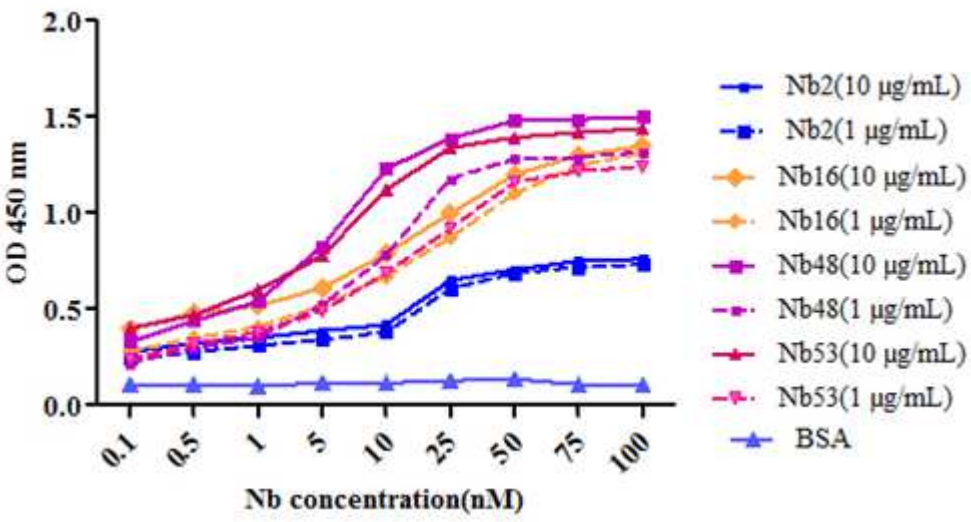

Figure 5. Affinity measurement. Affinity graph was represented based on Beatty ELISA method.

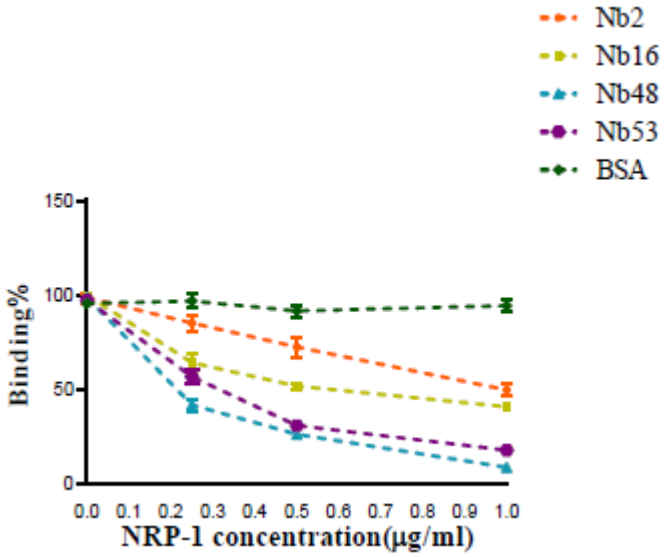

Figure 6. Competitive ELISA assay. Wells were coated with NRP-1 antigen, and the competitive binding of soluble nanobodies to immobilized NRP-1 and different amounts of soluble NRP-1was examined. BSA used as a negative controls. The data are presented as mean ±SD.

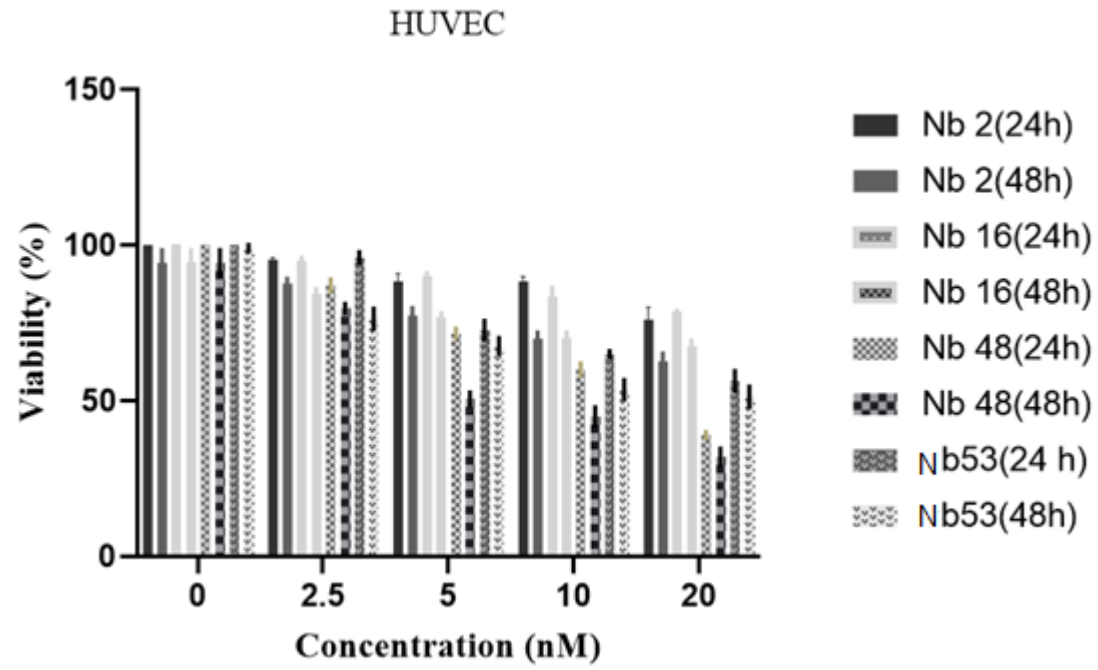

524

525

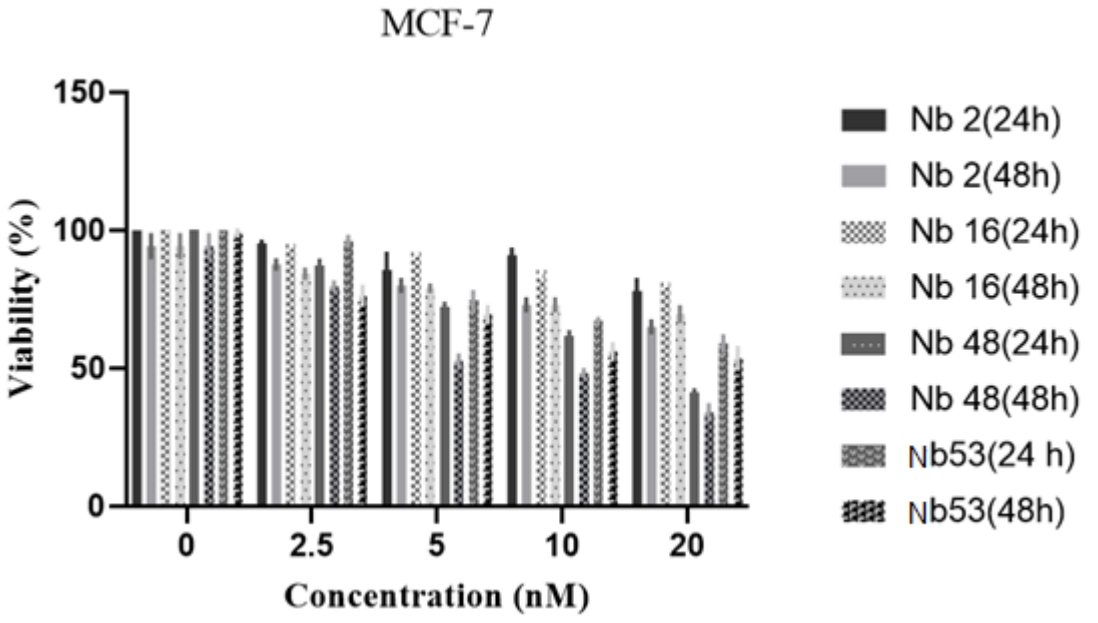

526

527

528

529 Figure 7. MTT Cell Proliferation Assay. MTT assay was performed for proliferation assay.
530 According to the figure, more than half of the HUVECs proliferation were inhibited in

presence of Nb48. Viability of MCF-7 was reduced by approximately 50% in case of Nb48 treatment. Data are expressed as mean ± SD

A 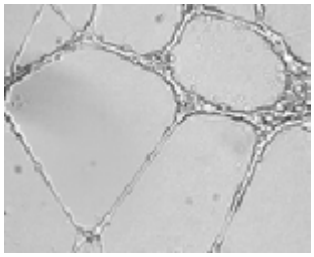 B 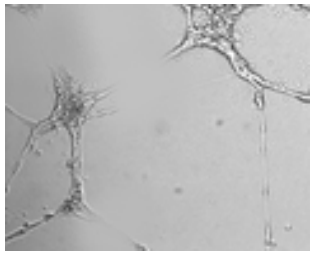

Figure8. Inhibition of NRP-1 receptor attenuates tube formation in HUVEC cells. Cells were incubated in the absence (A) or presence (B) of the Nb48. The data represent the means of three replicate ± SD ($p < 0.05$).

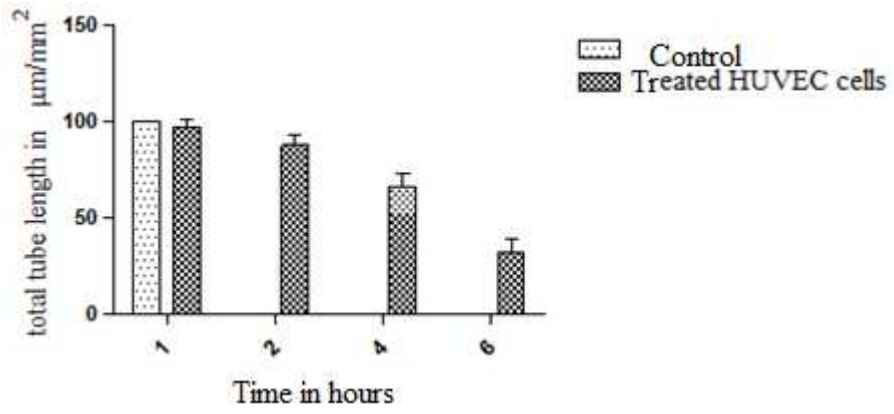

Figure9. Tube formation was inhibited by ~46% after 6h in presence of the 4nM of Nb48. Analysis was examined using Image J software.

A 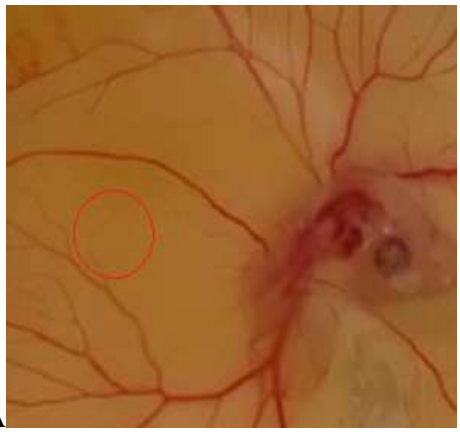 B 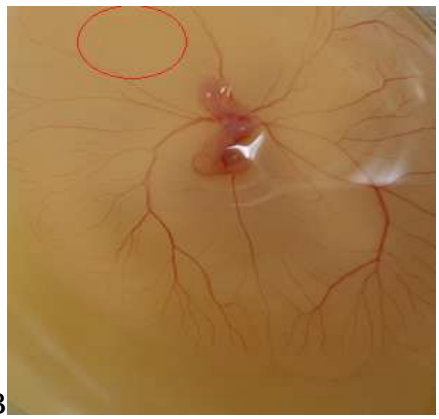

C 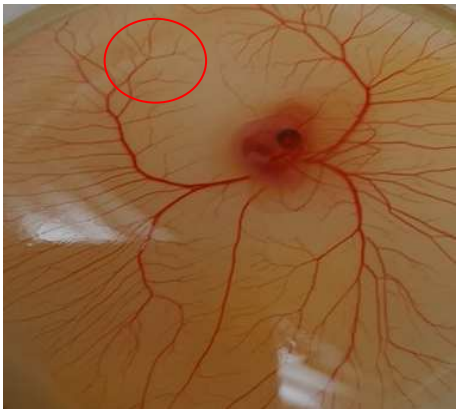

Figure10. CAM assay, (A): chick embryo in presence of 4nM/disc (after 24h) and (B) 4nM/disc (after 48h) containing of Nb48. (C) control (disc PBS).